

*Aleksandra Roszko*

AGH University of Science and Technology  
30 Mickiewicza Av., 30-059 Krakow, Poland, [roszko@agh.edu.pl](mailto:roszko@agh.edu.pl)

*Elzbieta Fornalik-Wajs*

AGH University of Science and Technology  
30 Mickiewicza Av., 30-059 Krakow, Poland, [elaf@agh.edu.pl](mailto:elaf@agh.edu.pl)

## POTENTIAL OF LOW CONCENTRATION NANOFLUIDS IN HEAT TRANSFER

### Abstract

The main purpose of conducted studies was recognition of low concentration nanofluid under the influence of magnetic field potential applications. The investigations are having fundamental character but Authors keep in mind better energy utilization through the heat transfer enhancement. The examined fluid was composed of water and Cu/CuO nanoparticles. Three temperature differences were imposed on the system. The results did not give unequivocal answer on possible utilization of studied phenomena, but there is open scene for the studies of particle-fluid interaction and flow structure. The main conclusion is that the magnetic properties of base fluid and particles are crucial for such analysis.

### Key words

weakly-magnetic nanofluid, heat transfer phenomena, strong magnetic field, thermo-magnetic convection

### Introduction

Nowadays, there are great numbers of electronic devices that surround us. Their proper operation depends on many factors, for example optimal temperature, humidity, cooling media, etc. The operational conditions are very important; therefore their selection and optimisation are significant [1]. From other point of view the energy itself is valuable. Many research subjects are related to its better utilization, more efficient devices or optimized systems [2-3]. The most important factor in the efficient energy usage corresponds to the efficient heat transfer. Traditional coolants have meaningful limitation, which is coming from their low thermal properties. There are many research works done on the heat transfer processes intensification [4-7]. Various passive and active methods are applied to augment the transfer of high heat fluxes. One of the passive methods resulted in an appearance of nanofluids. The idea of nanoparticles addition to the base fluid was born hundred years ago, but it was possible to realize it now due to the technological development. The first report on nanofluid successful preparation was published in 1995 [8]. Since then, interest in such fluids is constantly growing. There are more and more possible applications, among others: in solar systems [9], medicine [10] and in daily life [11-12]. Another way to enhance the heat transfer is application of the magnetic field. Several experimental and numerical studies were conducted [13-16]. It has been proven that the usage of an external, strong magnetic field could intensify or completely suppress the natural convection of one-phase paramagnetic fluid [17-18].

The demand of better energy utilization through the more efficient heat transfer was an origin of present investigations. Since the nanofluids and the magnetic field could enhance the processes, the idea of their combination seemed to be the logical consequence. However the cost of nanofluids is pretty high, therefore the low particle concentration fluids were firstly considered as the working media and the copper nanofluid was produced and studied. Although the results were different than expected, they have given insight on the phenomena occurring in the system. They can be explained through the forces acting on the base fluid and the particles. The reason was that the copper nanofluid turned to be copper oxide one. The difference in the magnetic properties caused very complex force system and difficulties in the results interpretation.

### Experimental setup and research methodology

Experimental equipment and enclosure are schematically shown in Fig.1. Experimental stand was consisted of an enclosure, filled with a working fluid, placed in the bore of a superconducting magnet, a heater control sys-

tem, a thermostating bath and a data acquisition system connected to a personal computer. To achieve the highest magnetic buoyancy force acting on the investigation system, the enclosure was placed at the location of  $\text{grad}B_{\text{max}}^2$  maximal value occurrence [18]. The bottom wall of the experimental enclosure was heated (with constant heat flux) and the top one was cooled, both of them were made of copper. A nichrome wire was used as a heater, connected to a DC power supply and placed under copper plate. The heating power was monitored with multimeters. The water flowing through the cooling chamber was maintained at constant temperature by a thermostating bath. Three thermocouples were placed in heated and cooled plates each, while six thermocouples inside cubical enclosure (shown in Fig. 1(b)). The signals of measured temperature were stored in a computer through a data acquisition system and were used to analyze the heat transfer and flow structure.

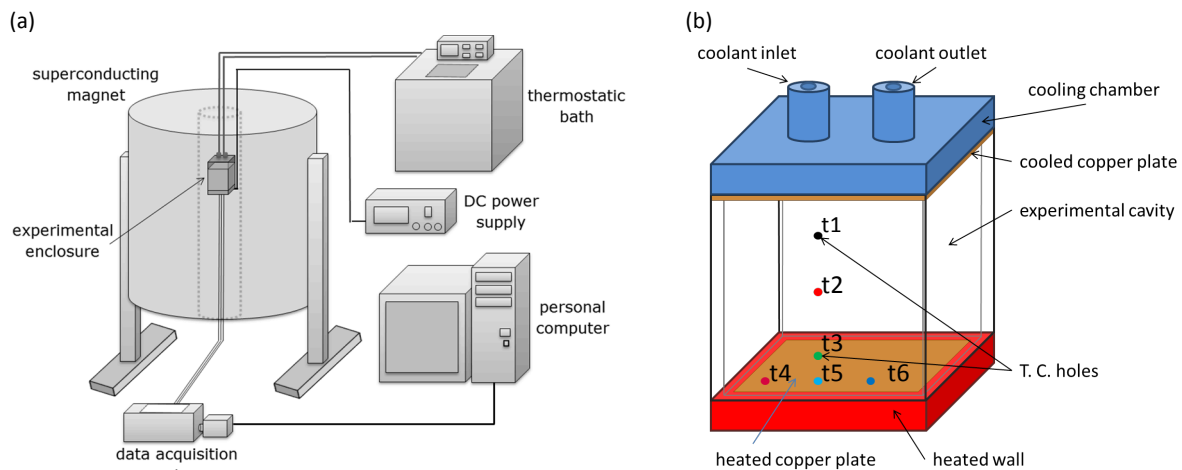


Fig. 1. Experimental (a) setup and (b) enclosure.  
Source: [16]

Table 1. Formulas applied for the calculation of nanofluids thermo-physical properties

Property	Formula
Thermalconductivity	$k_{nf} = k_{bf} \frac{k_p + 2k_{bf} + 2\varphi(k_p - k_{bf})}{k_p + 2k_{bf} - \varphi(k_p - k_{bf})}$
Density and specific heat product	$\rho c_{p,nf} = \varphi(\rho c_p)_p + (1 - \varphi)(\rho c_p)_{bf}$
Thermal expansion coefficient	$\beta_{nf} = \varphi\beta_p + (1 - \varphi)\beta_{bf}$
Dynamic viscosity	$\mu_{nf} = \frac{\mu_{bf}}{(1 - \varphi)^{2.5}}$
Electrical conductivity	$\sigma_{nf} = \sigma_{bf} \left[ 1 + \frac{3 \left( \frac{\sigma_p}{\sigma_{bf}} - 1 \right) \varphi}{\left( \frac{\sigma_p}{\sigma_{bf}} + 2 \right) - \left( \frac{\sigma_p}{\sigma_{bf}} - 1 \right) \varphi} \right]$

Source: [19]

Table 2. Thermo-physical properties of working fluids

Property	Unit	Value
Thermalconductivity	$k_{nf} [W \cdot (mK)^{-1}]$	0.601
Density	$\rho_{nf} [kg \cdot m^{-3}]$	1019
Specific heat	$c_{p,nf} [J \cdot (kg \cdot K)^{-1}]$	4177
Thermal expansion coefficient	$\beta_{nf} [K^{-1}]$	$19.78 \cdot 10^{-5}$
Dynamic viscosity	$\mu_{nf} [kg \cdot (m \cdot s)^{-1}]$	$10.07 \cdot 10^{-4}$
Electrical conductivity	$\sigma_{nf} [S \cdot m^{-1}]$	$5.52 \cdot 10^{-6}$
Mass magnetic susceptibility	$\chi_m [m^3 \cdot kg^{-1}]$	$12.4 \cdot 10^{-9*}$

Source: Authors - values calculated in the basis of Tab. 1, \* - measured values

Examined nanofluid consisted of distilled water with addition of 1% weight (corresponding to 0.112 vol.%) copper/copper oxide particles of 40-60 nm size. Nanofluid was prepared by a two-step method with ultrasonic agitation (Sonics & Materials Inc. model: VCX 130 PB, 130 W, 20 kHz) lasting about 10 minutes. The obtained liquid was opaque and stable for the duration of the experiment. To define the nanofluid thermo-physical properties the formulas listed in Table 1 were used. The magnetic susceptibility was determined experimentally. All properties applied in the analysis are presented in Table 2.

### The interaction of the gravitational and the magnetic buoyancy forces

The acting forces on the fluid (the gravitational and the magnetic buoyancy ones) can act in the same or in a different directions depending on some parameters. Thus, their mutual orientation, which effects on the total acting force, will be larger or smaller. Experimentally verified magnetic property of nanofluid indicated that it was diamagnetic (negative value of the magnetic susceptibility), therefore the maximal gradient of magnetic induction square was located on the cooling plate. Such arrangement should orient the forces in the same direction, and therefore the total acting force on the nanofluid should be higher. However added particles were paramagnetic and even they did not change much the bulk fluid magnetic susceptibility, the magnetic field was influencing them in different manner. Probably the additional force (magnetic buoyancy force for paramagnetics) appeared, what resulted in complex force system and the unequivocal results of the heat transfer. The schematic relationship of the force system is presented in Fig. 2.

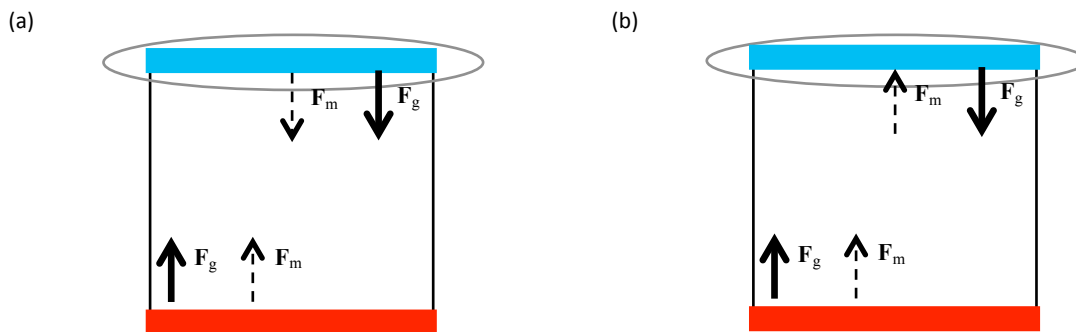


Fig. 2. Reciprocal relation of the gravitational ( $F_g$ ) and magnetic ( $F_m$ ) buoyancy forces for (a) diamagnetics and (b) paramagnetics.

Source: Authors

Values of the forces could be calculated by following formulas:

- the gravitational buoyancy force:

$$\mathbf{F}_g = -\mathbf{g}\rho_0\beta(T - T_0), \quad (1)$$

- the magnetic buoyancy force for diamagnetics:

$$\mathbf{F}_m = \frac{\chi_m\rho_0\beta(T - T_0)}{2\mu_0}\nabla\mathbf{B}_{\max}^2 \quad (2)$$

- the magnetic buoyancy force for paramagnetics:

$$\mathbf{F}_m = -\left(1 + \frac{1}{\beta T_0}\right) \frac{\chi_m\rho_0\beta(T - T_0)}{2\mu_0}\nabla\mathbf{B}_{\max}^2. \quad (3)$$

The  $T_0$  indicated reference temperature equal to the arithmetical average of cooled and heated walls' temperature.

Effect of magnetic field on heat transfer processes and flow structure is presented in Figs. 3-5.

### Signal analysis methodology

For each temperature difference methodology was the same. The first part of the analysis was related to the heat transfer and the first undertaken step was measurement of the conduction state to determine the heat loss in the system. Experimental enclosure was inverted in the position that the hot plate was at the top and cooled one at the bottom, then it was placed in the selected location in the magnetic field. The chosen test section corresponded to the place of maximum  $\text{grad}\mathbf{B}_{\max}^2$  occurrence. The ambient temperature in the magnet

was 18°C, therefore, cooled wall temperature was set at the same level and only the heated wall temperature could be changed. The next step was related to the measurement of convection state without and with magnetic field utilization. Taking into account convective and conducted heat fluxes, the Nusselt number could be defined:

$$\text{Nu} = \frac{Q_{\text{net\_conv}}}{Q_{\text{net\_cond}}} \quad (4)$$

According to the adopted assumption, that the heat loss would be the same regardless of the phenomenon occurring inside the enclosure, particular term could be calculated in the basis of following formulas:

$$Q_{\text{loss}} = Q_{\text{cond}} - Q_{\text{theor\_cond}} \quad (5)$$

$$Q_{\text{net\_conv}} = Q_{\text{conv}} - Q_{\text{loss}} \quad (6)$$

A linear dependence of heat losses on the temperature difference was obtained in the form:

$$Q_{\text{loss}} = 0.06398 \cdot \Delta T \quad (7)$$

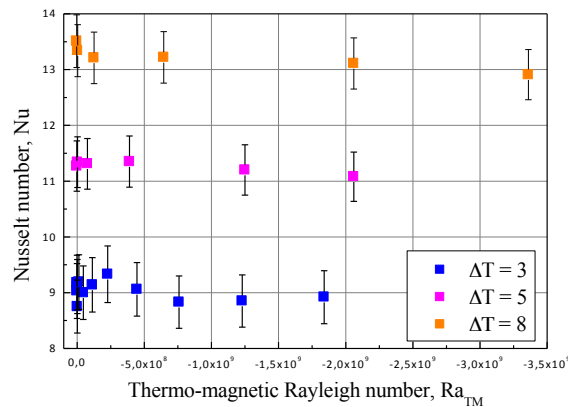
Knowing all of necessary components it was possible to calculate the Nusselt number.

The next part included the flow structure analysis with Fast Fourier Transformation utilization. Due to the nanofluid opaqueness there was no possibility to conduct an optical visualization. Therefore, the signal analysis using the FFT was the only way to get information about the flow structure. The results were demonstrating the peaks, which were associated with certain periodic phenomena. In the light of analyzed convection phenomenon a characteristic frequency could be interpreted as the occurrence of vortex structures. The FFT analysis was conducted with an algorithm presented in [20]. The representative results are shown in Figs. 4 and 5.

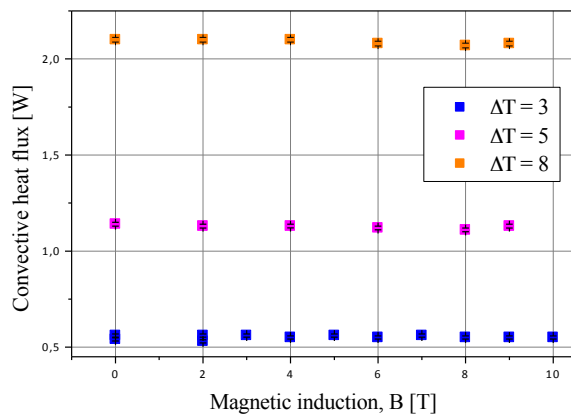
## Result discussion

In Fig. 3 (a) exemplary results of heat transfer analysis are shown. They are represented by the Nusselt number dependence on the thermo-magnetic Rayleigh number.

(a)



(b)



(c)

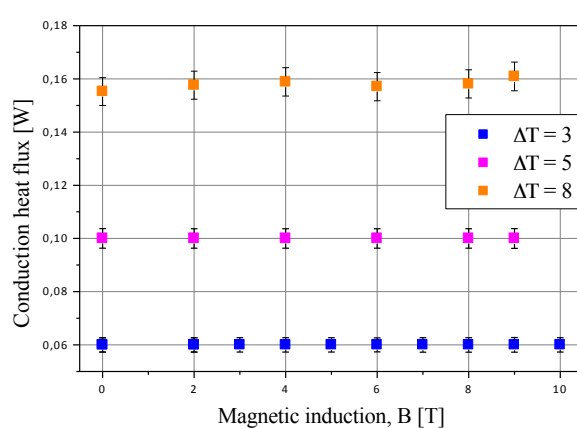


Fig. 3. (a) The Nusselt number versus the thermo-magnetic Rayleigh number; (b) convective and (c) conduction heat fluxes depended on the magnetic induction for various temperature differences.

Source: Authors

There is a clearly visible increase of the Nusselt number value at the magnetic induction up to 6T for the lowest temperature difference. However, at higher magnetic fields induction slight decrease of its value is observed. For higher temperature difference (5 degrees), increase of the Nusselt number is smaller, but still can be found. Whereas for the highest of examined temperature differences the Nusselt number decreased. The most likely, it could be explained by an increase of magnetic field influence on paramagnetic particles in nanofluid. The magnetic force was acting in the opposite way on the diamagnetic base fluid and the paramagnetic nanoparticles, at the upper part of the enclosure. Hence, with the increasing magnetic induction and the temperature difference an effect of paramagnetic nanoparticles became visible in the transport processes. The convective and conduction heat fluxes were analyzed for a better understanding of the issues in the corresponding temperature differences and shown in the Figs 3 (b) and (c). Convective heat flux did not change for the lowest temperature difference, while for the higher temperature difference a slight decrease at 6T of magnetic induction and its higher values could be observed. It should be noted that, the convective and conduction heat fluxes took higher values at the higher temperature differences, respectively. The conduction heat flux could be considered as almost constant, however with increasing magnetic induction it increased slightly for the highest temperature difference.

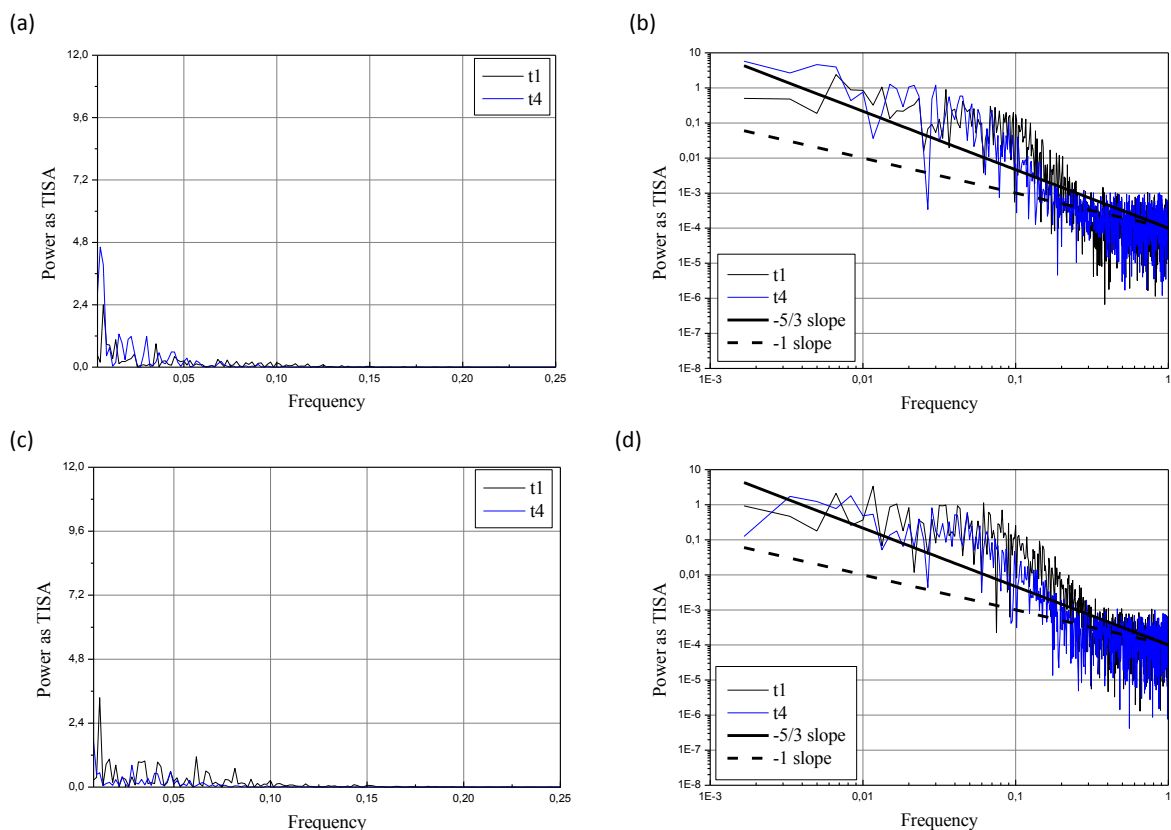


Fig. 4. The powerspectrum versus frequency (a) at 2T of magnetic induction,  $Ra_{TM} = -2.51 \cdot 10^6$ , (b) log-log scale at 2T of magnetic induction,  $Ra_{TM} = -2.51 \cdot 10^6$ , (c) at 6T of magnetic induction,  $Ra_{TM} = -3.90 \cdot 10^8$ , (d) log-log scale at 6T of magnetic induction,  $Ra_{TM} = -3.90 \cdot 10^8$ , for temperature difference of  $\Delta T = 5$ .

Source: Authors

Examples of spectral analysis as linear and log-log scale diagrams at 2T and 6T of magnetic induction are presented in Figs 4 and 5 for selected temperature differences, respectively. The various kind of power spectrum for 5 degrees of temperature difference are visible. The multiple peaks are shown at 2T of magnetic induction, which could indicate a multiscale structure of the swirls, while at 6T of magnetic induction the magnitude of the peaks is slightly smaller. The few clear peaks and many smaller ones are visible for 8 degrees of temperature difference at 2T of magnetic induction, which could point out on few large swirls and many small vortices present in the experimental enclosure. At higher value of magnetic induction the magnitude of peaks was reduced. Hence it could be stated that the increase of magnetic induction calmed down the fluid flow. The straight lines (-5/3 and -1 slopes) did not match the power spectrum distribution in any range for any present-

ed temperature difference, what suggested that the flow did not occur in the inertial-convective turbulent regime [21]. However, the change in nanofluids flow structure was noticeable.

On the basis of presented and all performed graphs and analyzes of the power spectrum versus frequency, it could be said that the magnetic field affected the flow structure and therefore energy transport within the nanofluid.

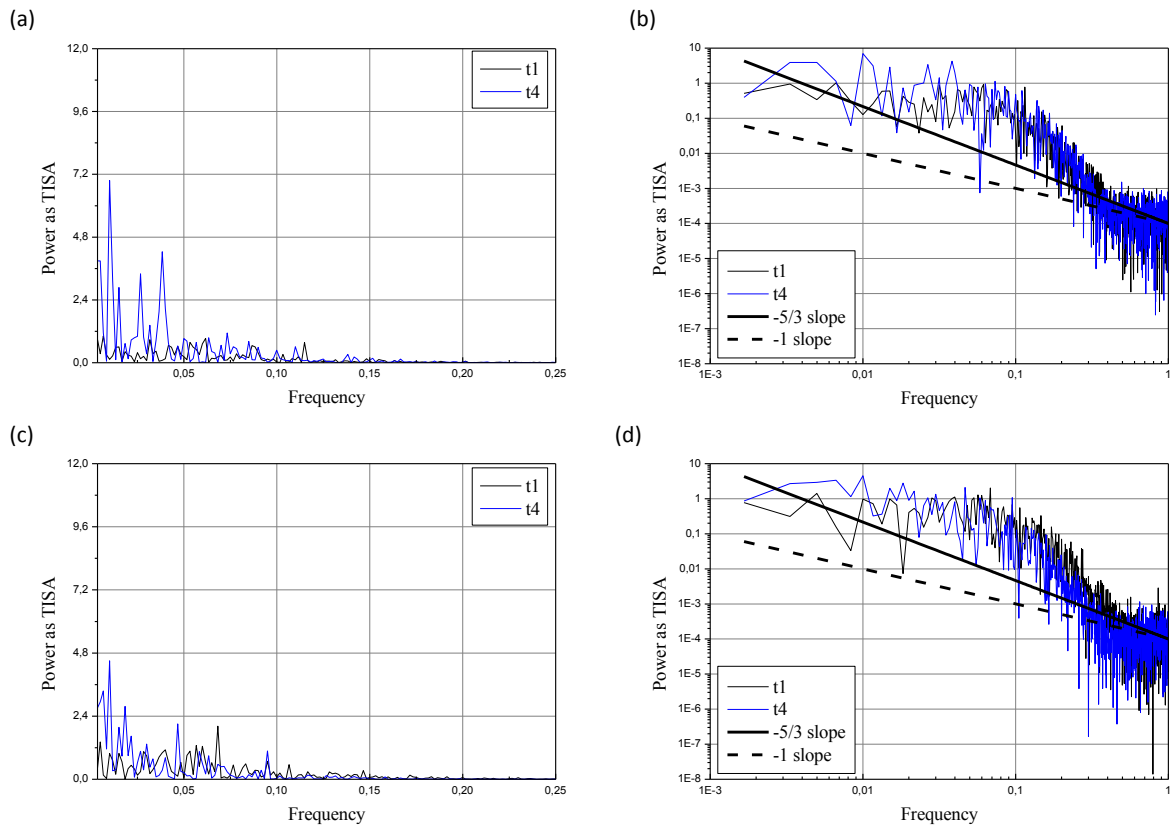


Fig. 5. The power spectrum versus frequency (a) at 2T of magnetic induction,  $Ra_{TM} = -4.09 \cdot 10^6$ , (b) log-log scale at 2T of magnetic induction,  $Ra_{TM} = -4.09 \cdot 10^6$ , (c) at 6T of magnetic induction,  $Ra_{TM} = -6.44 \cdot 10^8$ , (d) log-log scale at 6T of magnetic induction,  $Ra_{TM} = -6.44 \cdot 10^8$ , for temperature difference of  $\Delta T = 8$ .

Source: Authors

### Summary

In the paper the experimental analysis of thermo-magnetic convection of 0.112 vol.% Cu/CuO nanofluid was presented. The impact of magnetic field and various temperature differences on the heat transfer and the fluid flow structure was investigated. The recorded signal allowed analysis of the phenomena during the nanofluid thermo-magnetic convection. System of the gravitational and magnetic buoyancy forces, caused by different magnetic properties of base fluid and nanoparticles, was very complex. Therefore, the unequivocal answer on the question of potential utilization of low concentration nanofluid cannot be given. Such composition of nanofluid does not lead to a great effect, but it shows in which direction should go the next studies. In the next stage of study the nanofluids with the same magnetic properties of components will be considered to achieve the maximum magnetic field influence. Additionally, the interaction between fluid and particles in the magnetic field will be analyzed.

### Acknowledgements

The present work was supported by the Polish Ministry of Science (Grant AGH No. 15.11.210.307).

## Nomenclature

**B** - magnetic induction, T

$c_p$  - specific heat,  $J \cdot (kg \cdot K)^{-1}$

**F** - force,  $N \cdot m^{-3}$

**g** - gravitational acceleration,  $m \cdot s^{-2}$

**k** - thermal conductivity,  $W \cdot (m \cdot K)^{-1}$

$Q_{net\_cond}$  - conduction heat flux, W

$Q_{net\_conv}$  - convective heat flux, W

$Q_{loss}$  - heat loss flux, W

**Nu** - Nusselt number, dimensionless

**T** - temperature, K

$T_0$  - reference temperature, K

## Greek symbols

$\beta$  - thermal expansion coefficient,  $K^{-1}$

$\rho$  - density,  $kg \cdot m^{-3}$

$\mu$  - dynamic viscosity,  $kg \cdot (m \cdot s)^{-1}$

$\mu_0$  - magnetic permeability of vacuum,  $H \cdot m^{-1}$

$\sigma$  - electrical conductivity,  $S \cdot m^{-1}$

$\chi_m$  - mass magnetic susceptibility,  $m^3 \cdot kg^{-1}$

## Superscripts

bf - base fluid

g - gravitational buoyancy force

m - magnetic buoyancy force

nf - nanofluid

p - particles

## References

- [1] A. Ijam and R. Saidur, "Nanofluid as a coolant for electronic devices (cooling of electronic devices)," *Appl. Therm. Eng.* 32 (2012) 76–82
- [2] N. Putra, W. N. Septiadi, R. Sahmura, and C. T. Anggara, "Application of Al<sub>2</sub>O<sub>3</sub> Nanofluid on Sintered Copper-Powder Vapor Chamber for Electronic Cooling," *Adv. Mater. Res.* 789 (2013) 423–428
- [3] M. Rasponi, F. Piraino, N. Sadr, M. Laganà, A. Redaelli, and M. Moretti, "Reliable magnetic reversible assembly of complex microfluidic devices: fabrication, characterization, and biological validation," *Microfluid. Nanofluidics*, vol. 10, no. 5 (2010) 1097–1107
- [4] M. T. H. Mosavian, S. Z. Heris, S. G. Etemad, and M. N. Esfahany, "Heat transfer enhancement by application of nano-powder," *J. Nanoparticle Res.*, vol. 12, no. 7 (2010) 2611–2619
- [5] Y. Xuan and Q. Li, "Heat transfer enhancement of nanofluids," *Int. J. heat fluid flow* 21 (2000) 58–64
- [6] K. Khanafer, K. Vafai, and M. Lightstone, "Buoyancy-driven heat transfer enhancement in a two-dimensional enclosure utilizing nanofluids," *Int. J. Heat Mass Transf.*, vol. 46, no. 19 (2003) 3639–3653
- [7] D. Wen, G. Lin, S. Vafaei, and K. Zhang, "Review of nanofluids for heat transfer applications," *Particology*, vol. 7, no. 2 (2009) 141–150
- [8] S. U. S. Choi and J. A. Eastman, "Enhancing thermal conductivity of fluids with nanoparticles," 1995
- [9] R. S. Shawgo, A. C. Richards Grayson, Y. Li, and M. J. Cima, "BioMEMS for drug delivery," *Curr. Opin. Solid State Mater. Sci.*, vol. 6, no. 4, pp. 329–334, Aug. 2002.
- [10] O. Mahian, A. Kianifar, S. A. Kalogirou, I. Pop, and S. Wongwises, "A review of the applications of nanofluids in solar energy," *Int. J. Heat Mass Transf.*, vol. 57, no. 2, pp. 582–594, 2013.
- [11] Y. He, Y. Jin, H. Chen, Y. Ding, D. Cang, and H. Lu, "Heat transfer and flow behaviour of aqueous suspensions of TiO<sub>2</sub> nanoparticles (nanofluids) flowing upward through a vertical pipe," *Int. J. Heat Mass Transf.*, vol. 50, no. 11–12, pp. 2272–2281, 2007.

- [12] R. Taylor, S. Coulombe, T. Otanicar, P. Phelan, A. Gunawan, W. Lv, G. Rosengarten, R. Prasher, and H. Tyagi, "Small particles, big impacts: A review of the diverse applications of nanofluids," *J. Appl. Phys.*, vol. 113, no. 1 (2013) p. 011301
- [13] T. Bednarz, E. Fornalik, H. Ozoe, J. S. Szmyd, J. C. Patterson, and C. Lei, "Influence of a horizontal magnetic field on the natural convection of paramagnetic fluid in a cube heated and cooled from two vertical side walls," *Int. J. Therm. Sci.*, vol. 47, no. 6 (2008) 668–679
- [14] T. P. Bednarz, C. Lei, J. C. Patterson, and H. Ozoe, "Enhancing natural convection in a cube using a strong magnetic field — Experimental heat transfer rate measurements and flow visualization," *Int. Commun. Heat Mass Transf.*, vol. 36, no. 8 (2009) 97–102
- [15] E. Fornalik, P. Filar, T. Tagawa, H. Ozoe, and J. S. Szmyd, "Effect of a magnetic field on the convection of paramagnetic fluid in unstable and stable thermosyphon-like configurations," *Int. J. Heat Mass Transf.*, vol. 49, no. 15–16 (2006) 2642–2651
- [16] A. Roszko, E. Fornalik-Wajs, J. Donizak, J. Wajs, A. Kraszewska, and L. Pleskacz, "Magneto-thermal convection of low concentration nanofluids," *MATEC Web Conf.*, vol. 6, no. 18 (2014) 1–8
- [17] T. Bednarz, E. Fornalik, T. Tagawa, H. Ozoe, and J. S. Szmyd, "Experimental and numerical analyses of magnetic convection of paramagnetic fluid in a cube heated and cooled from opposing verticals walls," *Int. J. Therm. Sci.*, vol. 44, no. 10 (2005) 933–943
- [18] E. Fornalik, *Magnetic convection of paramagnetic fluid in an enclosure*. AGH Uczelniane Wydawnictwa Naukowo-Dydaktyczne, 2009
- [19] Y. Xuan and W. Roetzel, "Conceptions for heat transfer correlation of nanofluids," *Int. J. Heat Mass Transf.*, vol. 43 (2000) 3701–3707
- [20] <http://www.fft.w.org/>.
- [21] K. R. Sreenivasan, "The passive scalar spectrum and the Obukhov – Corrsin constant," *Phys. Fluids*, vol. 8 (1996) 189–196